quantitative analysis will be carried out here to clarify this point.

3.3 Instability of the Free Shear Layer

The Kelvin-Helmholtz instability was originally derived from two parallel stream of fluids with different velocity and density. Hence there are discontinuities in density and velocity at the interface. Chandrasekhar [22] considered the case of continuous variation of velocity and certain distribution of ρ (characterized by the Richardson number) and concluded from the inviscid linear stability analysis that, for any values of the Richardson number, there are always bands of wavelengths for which the Kelvin-Helmholtz instability occurs. In particular, when the Richardson number is zero, i.e. for constant density, the condition for the Kelvin-Helmholtz instability to occur is $0 < Kh < 1.2785$ where K is the wave number and h is the shear layer thickness. Both K and h can be extracted from LES data in the present study and for the semi-circular leading edge case $Kh = 0.984$ and for the blunt leading case $Kh = 1.1245$ (h is the shear layer thickness where the unsteadiness first becomes apparent and $K = 2\pi f/c$, f is the characteristic frequency which is obtained from the spectra analysis as shown in figure 5 and c is the wave speed equal to the velocity at the critical layer, i.e., the streamwise velocity at the inflection point). Hence it can be concluded that the free shear layer in both cases becomes unstable via the same instability, Kelvin-Helmholtz instability.

3.4 Vortex Shedding

It has been evident from experimental studies [3, 4, 5] that separated-reattached flows in a blunt leading edge are associated with vortex shedding and the measured average shedding frequency is about $0.6 – 0.7U_0/x_R$ (U_0 is the free stream velocity and x_R is the mean separation bubble length). In addition, there is a low frequency peak according to the experimental data. Figure 5 presents the velocity spectra for the semi-circular leading edge and the blunt leading edge cases and it can be seen clearly that there is a peak band of frequencies for both cases, not periodic in the sense that there is only a single frequency. The shedding process occurs within a narrow band of frequencies and for the semi-circular leading edge case the predicted average frequency can be estimated at about $0.74U_0/x_R$. For the blunt leading edge case the predicted average frequency is about $0.78U_0/x_R$, both values are close to the experimental data, indicating that the simulations capture the flow physics of vortex shedding well and also confirm that the shedding process in both cases are very similar. The low frequency peak observed in many experimental studies are not apparent in the present study although in the semi-circular leading edge case a low frequency peak band was visible further upstream as shown in figure 6 and an explanation was given regarding how it happens [9]. However, this low frequency has not been observed in the LES studies for the blunt leading edge case [7, 8] and further investigation is needed in this area to fully understand this phenomenon.

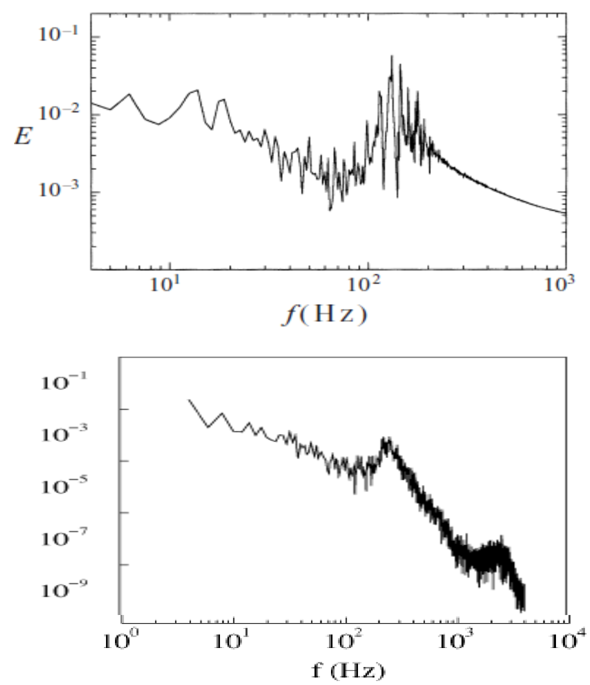

Fig. 5 Velocity spectra, above: semi-circular leading edge at $x/x_R = 0.7$ and $y/x_R = 0.04$; below: blunt leading edge at $x/x_R = 0.5$ and $y/x_R = 0.13$.

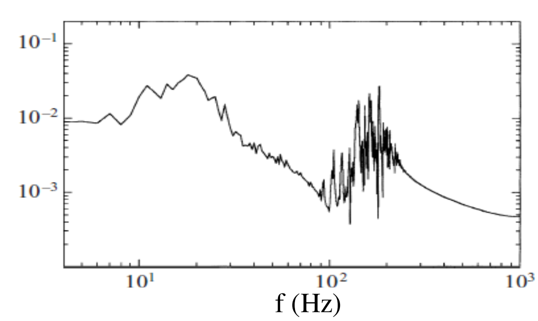

Fig. 6 Power spectrum of u' at $x/x_R = 0.35$ and $y/x_R = 0.04$ for the semi-circular leading edge case.

3.5 Large-Scale Vortex Structures

It has been well established that large scale structures, usually called coherent structures, exist in many transitional and turbulent flows. The topology and range of scales of those large scale structures vary from flow to flow such as counter-rotating vortices in wake flows, streaks and hairpin vortices in turbulent boundary layer. In the present study the flow visualisation reveals various kinds of large scale 2D and 3D structures as shown in figure 7.

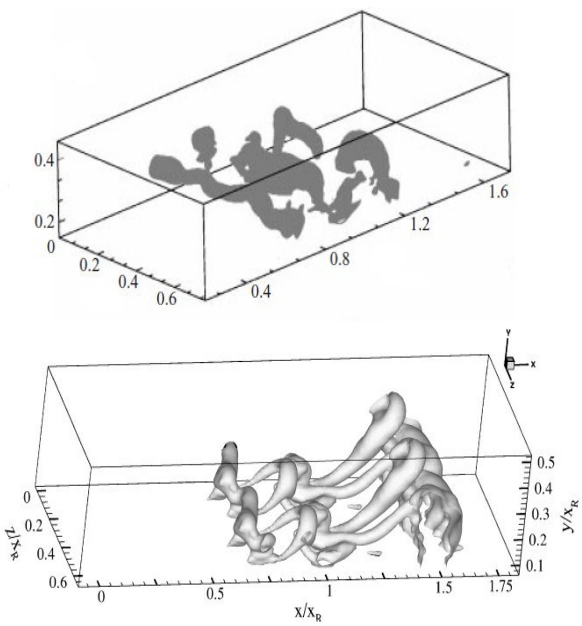

Fig. 7 Low-pressure iso-surfaces showing the transformation of Kelvin-Helmholtz rolls into hairpin or Λ-shaped vortices, above: semi-circular leading edge; below: blunt leading edge.

The free shear layer becomes unstable due to Kelvin-Helmholtz instability and the two-dimensional Kelvin-Helmholtz rolls are shed downstream of the plate leading edge and become distorted as they travel downstream. The Kelvin-Helmholtz rolls are subjected to approximately sinusoidal undulation (waviness) along the spanwise. It can clearly be seen that the axis of the the spanwise rolls remains perpendicular to the flow direction thus keeping their coherency and two-dimensionality nature up to a certain distance downstream. Further downstream the above described 2D spanwise coherent vortical structures become more distorted (specially the initially shed roll) leading to the appearance of a well-organised array of streamwise vortices originating from the initially shed vortical tube, and transform into three-dimensional vortical structures called Λ-vortices as shown in figure 7. This process is quite similar in both cases.

The 2D Kelvin-Helmholtz rolls can be transformed into 3D vortical structures called Λ-vortices as shown in figure 7. However it is also possible that those 2D rolls can be transformed into another form of 3D vortical structures called ribs [23] as shown in figure 8 below. It can be seen from these figures that the Kelvin-Helmholtz rolls have been transformed into streamwise ribs connecting a totally distorted and torn apart spanwise vortical structures. It is quite tempting to assume that these ribs are actually originating from Lambda-shaped vortices which are subjected to more stretching along the axial direction leading to the disintegration of its legs.

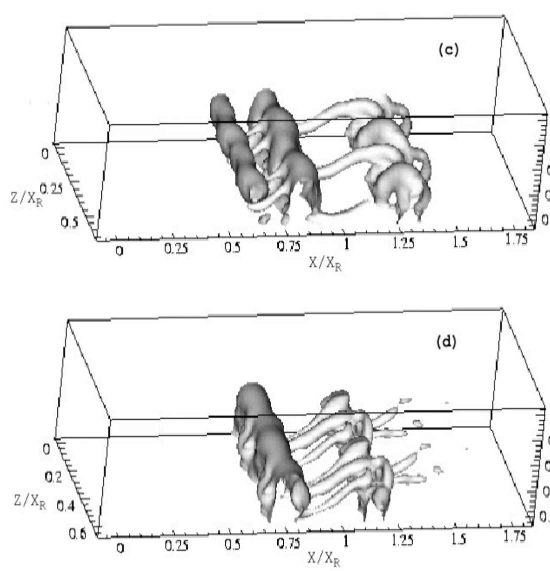

Fig. 8 Low-pressure iso-surfaces displaying the transformation of 2D Kelvin-Helmholtz rolls into streamwise large-scale vortical structures called ribs for the blunt leading edge case.

The transition process is usually very complicated and can follow many possible routes. For attached boundary layer transition the transition process can be divided into the following several stages [24]:

1). Receptivity stage – how the disturbances are projected into growing eigenmodes, or how they enter or otherwise induce disturbances in a boundary layer.

2). Linear growth stage (primary instability) – small disturbances are amplified till they reach a size where nonlinear growth starts. This amplification can be in the form of exponential growth of eigenmodes, nonmodal growth of optimal disturbances, or nonmodal responses to forcing.

3). Secondary instability – Usually once a disturbance reaches a finite amplitude it often saturates and transform the flow into a kind of new, possibly steady state. Very rarely the primary instability can lead the flow directly in a turbulent state and the new steady or quasi-steady flow becomes a base on which secondary instability can occur. This secondary instability can be viewed as a new instability of a more complicated flow.

4). The breakdown stage – nonlinearities and possibly higher instabilities excite an increasing number of scales and frequencies in the flow. This stage is more rapid than both the linear stage and the secondary instability stage.

However, for the separated boundary layer flow the transition process is less well understood compared with the attached boundary layer transition. It is proposed [6] that this transformation of the Kelvin-Helmholtz rolls into the three-dimensional vortical structures is likely due to a secondary instability, the helical pairing instability, which is a kind of two-dimensional subharmonic Eckhaus-type secondary instability [24]. The result is the growth of a disturbance with twice the wavelength of the initial vortices, producing a pairing of two vortices into a row of vortices, which can be seen from figure 9.

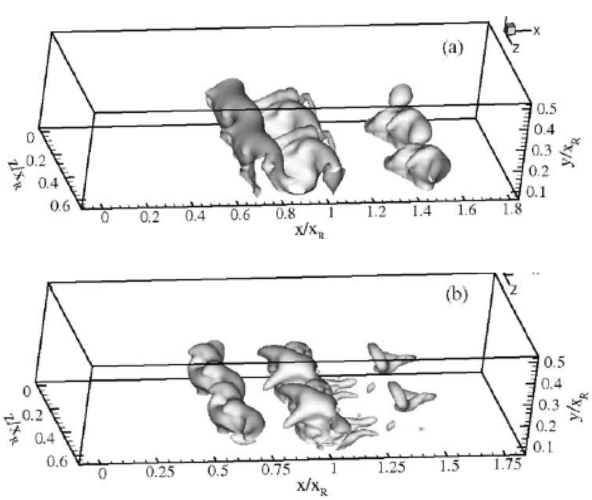

Fig. 9 Pairing of 2D Kelvin-Helmholtz rolls, indicating a kind of 2D subharmonic secondary instability for the blunt leading edge case.

Another possibility is that the 2D Kelvin-Helmholtz vortices can experience the so called three-dimensional elliptic-type secondary instability [24] and the result is the growth of spanwise disturbances on the 2D vortices in conjunction with the appearance of secondary streamwise vortices connecting the original spanwise vortices. Once the three-dimensional disturbance reaches a finite amplitude it leads to a bending of the core of the 2D vortices in the streamwise direction, eventually resulting in the so called rib vortices as shown in figure 8. It is not entirely clear which secondary instability is more dominant as both the pairing of vortices and the rib vortices have been observed in the present study, especially in the blunt leading edge case and further study is needed to clarify this point.

The breakdown stage occurs around the reattachment point and it happens rapidly as mentioned above, associated with irregular vortex shedding and the instantaneous reattachment point is moving upstream and downstream greatly. The instantaneous reattachment point can move about 50% of the mean bubble length. Immediately after the reattachment point a turbulent boundary layer forms quickly but it takes a quite long distance downstream for the log law and inner turbulence structures to develop as reported by many studies [25, 26, 27]. Since the final stage of breakdown is very complicated and involves strong nonlinearities and possibly higher instabilities so that both experimental and theoretical studies have their limitations and the most promising tools to study this is numerical simulations.

4 Conclusion

This paper presents a comparative study of transition process of a separated boundary layer on a flat plate with two different leading edges (blunt and semi-circular). The entire transition process, starting from initial instability in the free shear layer of the separation bubble and eventually leading to breakdown to turbulence has been visualized for both cases. It can be seen clearly that transition processes in both case are very similar with similar two-dimensional Kelvin-Helmholtz rolls and three-dimensional vortical structures (Λ-vortices) observed at various stages of the transition process in both cases. From detailed quantitative analysis of the LES data it has been shown that the free shear layer formed in the separation bubble is inviscidly unstable via the Kelvin-Helmholtz instability mechanism in both cases. These initial two-dimensional instability waves grow downstream linearly, with slow development of three-dimensional motions via possibly a secondary instability mechanism responsive to any small spanwise disturbance. Further downstream the distorted spanwise two-dimensional vortices roll up, leading to the formation of three-dimensional vortical structures. Breakdown to turbulence occurs around the mean reattachment point and the flow develops into a turbulent boundary layer rapidly after the reattachment.

Similar vortex shedding from the separated free shear layer has been observed in both cases. This is not periodic in the sense that a unique frequency exists, and the predicted average characteristic shedding frequencies in both cases are close to the measured value indicating that the numerical simulations have captured the flow physics well. Nevertheless the low frequency peak observed in several experimental studies of separated flow over a blunt plate is not apparent in the simulations.

The transformation of two-dimensional Kelvin-Helmholtz rolls into three-dimensional vortical structures may be due to a secondary instability, a kind of two-dimensional subharmonic Eckhaus-type secondary instability or a three-dimensional elliptic-type secondary instability, and further studies are needed to clarify this. Other factors which can influence the transition process in a separated boundary layer such as free stream turbulence have not been discussed at all in the present paper. The final breakdown stage to turbulence is far from fully understood and further research in this area is much needed.

Acknowledgment: The author gratefully acknowledges that some of the results presented in this paper were produced by Dr. I.E. Abdalla during his Ph.D study under my supervision.

References:

[1] R.B. Langtry and F.R. Menter, Transition Modelling for General CFD Applications in Aeronautics, *AIAA 2005-522, Reno, Nevada*.

[2] J. Smagorinsky, General Circulation Experiments with the Primitive Equations: I – the Basic Experiment, *Monthly Weather Review*, Vol. 91, 1963, pp. 99-164.

[3] M. Kiya, K. Sasaki, Structure of a Turbulent Separation Bubble, *Journal of Fluid Mechanics*, Vol. 137, 1983, pp. 83-113.

[4] M. Kiya, K. Sasaki, Structure of Large-scale Votices and Unsteady Reverse Flow in the Reattaching Zone of a Turbulent Separation Bubble," *Journal of Fluid Mechanics*, Vol. 154, 1985, pp. 463-491.

[5] N. J. Cherry, R. Hillier, M. P. Latour, Unsteady Measurements in a Separated and Reattaching Flow, *Journal of Fluid Mechanics*, Vol. 144 1984, , pp. 13-46.

[6] I. E. Abdalla, Z. Yang, 'Numerical Study of the Instability Mechanism in Transitional Separating - Reattaching Flow, *International Journal of Heat and Fluid Flow*, Vol. 25, 2004, pp 593-605.

[7] I. E. Abdalla, Z. Yang, Numerical Study of a Separated-Reattached Flow on a Blunt Plate", *AIAA Journal*, Vol. 43, 2005, pp 2465-2474.

[8] Z. Yang, I. E. Abdalla, Effects of Free-Stream Turbulence on a Transitional-Reattached Flow over a Flat Plate with a Sharp Leading Edge," *International Journal of Heat and Fluid Flow*, Vol. 30, 2009, pp 1026-1035.

[9] Z. Yang, P. R. Voke, Large-eddy simulation of boundary layer separation and transition at a change of surface curvature, *Journal of Fluid Mechanics*, Vol. 439, 2001, pp. 305-333.

[10] V. S. Djanali, K.C. Wong, S.W. Armfield, Numerical Simulations of Transition and Separation on a Small Turbine Cascade, *WSEAS Transactions on Fluid Mechanics*, Vol. 1, 2006, pp. 879-884.

[11] M. Ubaldi, P. Zunino, Transition and Loss Generation in the Profile Boundary Layer of a Turbine Blade, *WSEAS Transactions on Fluid Mechanics*, Vol. 1, 2006, pp. 779-784.

[12] P. Sagaut, *Large Eddy Simulation for Incompressible Flows*, 2nd edition, Springer, 2002.

[13] M. Lesieur, O. Metais, P. Comte, *Large-Eddy Simulation of Turbulence,* Cambridge University Press, 2005.

[14] E. Garnier, P. Sagaut, N. Adams, *Large Eddy Simulation for Compressible Flows*, Springer, 2009.

[15] S. A. Jordan, Large-Eddy Simulation Methodology in Generalized Curvilinear Coordinates, *Journal of Computational Physics*, Vol. 148, 1999, pp. 322-340.

[16] Z. Yang, Large Eddy Simulation of Fully Developed Turbulent Flow in a Rotating Pipe, *International Journal for Numerical Methods in Fluids*, Vol. 33, 2000, pp. 681-694.

[17] Z. Yang, P. R. Voke, Large-Eddy Simulation of Separated Leading-Edge Flow in General Co-ordinates, *International Journal for Numerical Methods in Engineering*, Vol. 49, 2000, pp. 681-696.

[18] K. Mahesh, G. Constantinescu, P. Moin, A Numerical Method for Large-Eddy Simulation in Complex Geometries, *Journal of Computational Physics*, Vol. 197 2004, pp. 215-240.
[19] M. Lesieur, O. Metais, New Trends in Large Eddy Simulations of Turbulence, *Annual Review of Fluid Mechanic,* Vol. 28, 1996, pp. 45-82.
[20] T. Kajishima, T. Nomachi, One-Equation Sub-grid Scale Model Using Dynamic Procedure for the Energy Production, *Transaction of ASME*, Vol. 73, 2006, pp. 368-373.
[21] P. Germano, U. Piomelli, P. Moin, W. H. Cabot, A Dynamic Sub-grid Scale Eddy Viscosity Model, *Physics of Fluids,* Vol. 3, 1991, pp. 1760-1765.
[22] S. Chandrasekhar, *Hydrodynamic and Hydromagnetic Stability*, Clarendon, 1961.
[23] Z. Yang, I.E., Abdalla, On Coherent Structures in a Separated/Reattached Flow, *WSEAS Transactions on Fluid Mechanics*, Vol. 3, 2008, pp. 143-153.
[24] P.J. Schmid, D.S. Henningson, *Stability and Transition in Shear Flows*, Springer, 2001.
[25] P. Bradshaw, F.Y.F, Wong, 1972 The Reattachment and Relaxation of a Turbulent Shear Layer, *Journal of Fluid Mech*anics, Vol. 52, 1972, pp. 113-135.
[26] M. Alam, N.D. Sandham, Direct Numerical Simulation of `Short' Laminar Separation Bubbles with Turbulent Reattachment, *Journal of Fluid Mech*anics, Vol. 410, 2000, pp. 1-28.
[27] I. Castro, E. Epik, Boundary Layer Development after a Separated Region, *Journal of Fluid Mech*anics, Vol. 374, 1998, pp. 91-116.